ACS APPLIED MATERIALS & INTERFACES

Research Article

www.acsami.org

Synthesis and Characterization of Magnetic Iron Oxide/Calcium Silicate Mesoporous Nanocomposites as a Promising Vehicle for Drug Delivery

Bing-Qiang Lu,[†] Ying-Jie Zhu,*[,†] Hai-Yong Ao,[‡] Chao Qi,[†] and Feng Chen[†]

[†]State Key Laboratory of High Performance Ceramics and Superfine Microstructure, Shanghai Institute of Ceramics, Chinese Academy of Sciences, Shanghai 200050, P. R. China

[‡]Key Laboratory of Inorganic Coating Materials, Shanghai Institute of Ceramics, Chinese Academy of Sciences, Shanghai 200050, P. R. China

Supporting Information

ABSTRACT: The synthesis of the mesoporous nanocomposites consisting of magnetic iron oxide nanoparticles and calcium silicate with uniform size has been a challenge, although they are the ideal potential agent for medical diagnosis and therapy. In this work, the core/shell structured mesoporous nanocomposites consisting of magnetic iron oxide nanoparticles as the core and calcium silicate as the shell have been successfully synthesized using a two liquid phase system by ultrasound irradiation, in which the hydrophobic phase is composed of hydrophobic Fe_3O_4 nanoparticles and tetraethyl orthosilicate (TEOS), and the water phase consists of $Ca(NO_3)_2$, NaOH, and water. The hollow mesoporous nanocomposites consisting of magnetic iron oxide nanoparticles and calcium silicate are obtained by adding a certain amount of the inert hydrophobic solvent isooctane in the reaction system before ultrasound irradiation. The nanocomposites have a superparamagnetic behavior, high Brunauer–Emmett–Teller (BET) specific surface area (474 $m^2\ g^{-1}$), and high Barrett–Joyner–Halenda (BJH) pore volume (2.75 $cm^3\ g^{-1}$). The nanocomposites have high drug loading capacities for bovine hemoglobin, docetaxel, and ibuprofen. The docetaxel-loaded nanocomposites have the anticancer ability and, thus, are promising for applications in biomedical fields.

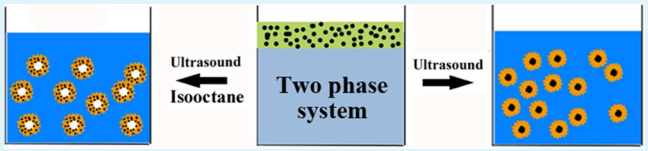

KEYWORDS: *iron oxide, calcium silicate, mesoporous materials, nanocomposites, core–shell, drug delivery, magnetic*

INTRODUCTION

Magnetic iron oxides (MIO), e.g., Fe_3O_4 and γ-Fe_2O_3, have wide potential applications in medical diagnosis and therapy, such as magnetic resonance imaging, hyperthermia, magnetic separation, and targeted drug delivery, due to their magnetism and biocompatibility.[1] MIO particles with different sizes (nanometers to micrometers) and surface properties (hydrophilic and hydrophobic) have been successfully synthesized.[2] As a result of the low specific surface areas of MIO particles synthesized by the conventional methods, their application in drug delivery is limited by the low drug loading capacity. To solve this problem, mesoporous MIO nanoparticles with polymers modifying the surface[3] and nanocomposites of MIO and other components (NMOC) (e.g., silica, calcium phosphate, and polymers) were synthesized.[4−10] Among various NMOC, the core–shell nanocomposites with mesoporous silica coating the MIO have been extensively studied in the past years. The silica shell thickness can be easily tuned, and the mesopores are formed using surfactants as the pore-forming agents.[4] However, the residual surfactants may cause cytotoxicity, and the pore diameters are generally small (below 5 nm); only drug molecules with low molecular mass can be loaded into the pores.[11] As to NMOC formed with calcium phosphate, although the drug loading capacity can be enhanced, the morphologies are rarely uniformly formed, owing to the challenge in controlling the growth of calcium phosphate.[5,7] Preparing NMOC with polymers can also increase the drug loading capacity as polymers generally possess various organic groups which can strongly adsorb drug molecules, whereas the safety and biodegradability of some polymers are still unclear. Therefore, the synthesis of NMOC for effective and safe biomedical applications is still a challenge.

Calcium silicates (CSs) have attracted increasing attention in the biomedical field in the past years. The excellent bioactivity and biodegradability compared with other inorganic biomaterials, such as Au and silica, have made CSs promising materials in bone repair. Besides, the application of CSs in drug delivery was also reported.[12−15] Until now, CS nanostructured materials have not been successfully used to construct the targeted drug carrier. For one thing, the relative inert surface is not suitable for functionalizing CS with ligands, peptides, or oligonucleotides to reach target cells and tissues. For another, CS can hardly form uniform nanocomposites with magnetic agents to

Received: September 27, 2012
Accepted: November 26, 2012
Published: December 4, 2012

construct magnetic targeted drug carriers. Take the core−shell structure with CS coating the MIO for example, the sheet-like structure of CS prepared by conventional methods makes it a big challenge to coat on the core with a closed shell. However, considering the advantages of MIO and CS, the nanocomposites consisting of these two constituents should be the ideal agents in medical diagnosis and therapy. Therefore, great efforts should be exerted to develop NMOC constructed by MIO nanoparticles and CS.

For the first time, we present a simple way to prepare mesoporous magnetic iron oxide/calcium silicate nanocomposites (MMCNs). The mesoporous nanocomposites consist of magnetic iron oxide nanoparticles as the core and calcium silicate as the shell. The MMCNs have the following features: superparamagnetic behavior, high specific surface area, large pore volume, high drug loading capacity for ibuprofen, docetaxel, and hemoglobin, and anticancer ability. The MMCNs are synthesized with the aid of ultrasound in a reaction system of two liquid phases. The hydrophobic phase is composed of hydrophobic Fe_3O_4 nanoparticles, tetraethyl orthosilicate (TEOS), and an inert hydrophobic solvent (e.g., isooactane, not essential). The water phase consists of $Ca(NO_3)_2$, NaOH, and water. Under the ultrasonic irradiation, the two liquid phases are mixed, and the MMCNs are formed after a heterogeneous reaction. The hollow mesoporous nanocomposites consisting of magnetic iron oxide nanoparticles and calcium silicate are obtained by adding a certain amount of the inert hydrophobic solvent isooctane in the reaction system before ultrasound irradiation. The mesoporous nanocomposites are promising for the applications in biomedical fields.

EXPERIMENTAL SECTION

Chemicals. All chemicals used in the experiments were purchased and used without further purification. Analytical grade reagents of $Ca(NO_3)_2{\cdot}4H_2O$, oleic acid, and tetraethyl orthosilicate (TEOS) were purchased from Sinopharm Chemical Reagent Co., Ltd. Magnetic iron oxide (Fe_3O_4, MIO) nanoparticles (about 13.8 nm in diameter) were purchased from Aladdin Reagents Corporation. Ibuprofen (99.95%) was purchased from Shanghai Yuanji Chemical Co., Ltd. Docetaxel (>98%) and bovine hemoglobin (~64 500 Da) were purchased from Sangon Biotech Corporation (China). Deionized water was used in all experiments.

Synthesis of Mesoporous Magnetic Iron Oxide-Calcium Silicate Nanocomposites (MMCNs). The MIO nanoparticles were first modified with oleic acid. Typically, MIO nanoparticles (1.000 g) and oleic acid (0.500 g) were added into ethanol (100 mL), and the mixture was treated with ultrasound for 10 min. Then, after 10 min, the big MIO nanoparticles deposited on the bottom, and the MIO−ethanol colloid solution was centrifuged. The product was washed with ethanol several times and dried at 60 °C.

The MMCNs were synthesized with the aid of ultrasound in a two liquid phase system. The oleic acid-modified MIO nanoparticles (0.0502 g) were dispersed in TEOS (0.68 mL) using ultrasound. Then, $Ca(NO_3)_2{\cdot}4H_2O$ aqueous solution (0.0477 mol L^{-1}, 125 mL) was added to form the two phase system, in which the hydrophobic phase containing MIO nanoparticles and TEOS floated on the $Ca(NO_3)_2{\cdot}4H_2O$ aqueous phase. The mixture was irradiated with the ultrasonic wave (200 W, 20 kHZ) using a high-intensity ultrasonic probe (Scientz, JY92-2D, Ti-horn) for 20 min. When it was irradiated for 2 min, NaOH solution (2.000 mol L^{-1}, 5 mL) was added, and the white $Ca(OH)_2$ formed and began to react with TEOS. After the ultrasound irradiation, the product was separated with a magnet, washed with water and ethanol several times, and dried at 60 °C.

To investigate the influence of the hydrophobic phase on the product, the inert organic solvent isooctane (0.3 or 0.6 mL) was added into the hydrophobic phase before mixing with $Ca(NO_3)_2{\cdot}4H_2O$ aqueous solution. During the synthesis of the MMCNs in the presence of isooctane, we found that a part of the hydrophobic phase attached on the container wall and more time was needed for complete reaction. To solve this problem, we stirred the reaction system for 3 s in every 30 s with a glass rod and extended the irradiation time to 24 min. Other experimental conditions were kept the same as above.

Drug Loading and In Vitro Release. MMCNs synthesized using a two liquid phase system by ultrasound irradiation in the absence of isooctane were used as the drug carrier. Docetaxel, ibuprofen (small molecular mass), and bovine hemoglobin (high molecular mass) were used as the model drugs. The chemical structures of docetaxel and ibuprofen are shown in Scheme 1.

Scheme 1. Chemical Structures of Docetaxel and Ibuprofen

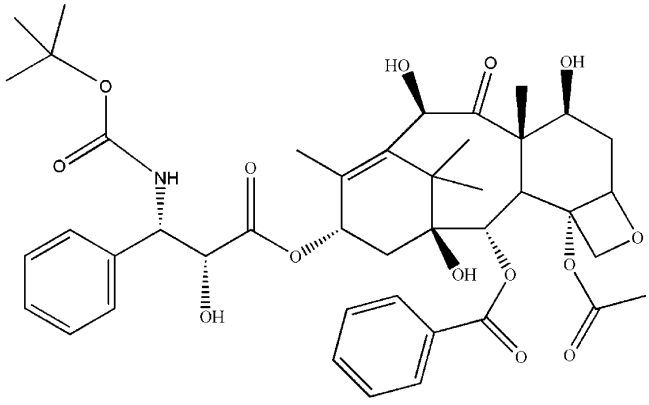

Docetaxel

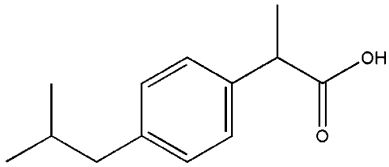

Ibuprofen

Loading Docetaxel. The MMCNs (0.0998 g) were mixed with 10 mL of docetaxel−ethanol solution (40 mg mL^{-1}). The mixture was treated with ultrasound for 3 min, sealed to prevent ethanol evaporation, and oscillated for 24 h (140 rpm, 37 °C). The drug loaded MMCNs were separated by centrifugation and dried at 37 °C. The supernatant was analyzed with a UV−vis spectrophotometer (Techcomp, UV2300) at the wavelength of 228 nm to determine the drug loading capacity.

In Vitro Docetaxel Release. The dried docetaxel-loaded MMCNs (5.0 mg) were immersed in phosphate buffer saline (PBS, pH = 7.4, 10 mL), shaken at the constant rate of 140 rpm (37 °C). At given time points, 0.4 mL of release medium was extracted for analysis, and 0.4 mL of fresh PBS was added into the release system to keep the same volume of release medium. 0.2 mL of release medium extracted from the release system was mixed with 0.2 mL of ethanol and analyzed with a UV−vis spectrophotometer (Techcomp, UV2300) at the wavelength of 230 nm to determine the concentration of docetaxel in the release system.

Loading Ibuprofen. The MMCNs (0.050 g) were mixed with 10 mL of ibuprofen−hexane solution (40 mg mL^{-1}). The mixture was treated with ultrasound for 3 min, sealed to prevent hexane evaporation, and oscillated for 24 h (140 rpm, 37 °C). The drug loaded MMCNs were separated by centrifugation and dried at 37 °C. The supernatant was analyzed with a UV−vis spectrophotometer

(Techcomp, UV2300) at the wavelength of 263 nm to determine the drug loading capacity.

Loading Bovine Hemoglobin. The MMCNs (0.050 g) were mixed with 10 mL of bovine hemoglobin aqueous solution (3.0 mg mL^{-1}). The mixture was treated with ultrasound for 3 min, sealed, and oscillated for 4 h (140 rpm, 37 °C). The drug loaded MMCNs were separated by centrifugation and dried at 37 °C. The supernatant was analyzed with a UV−vis spectrophotometer (Techcomp, UV2300) at the wavelength of 406 nm to determine the drug loading capacity.

In Vitro Cytotoxicity of Docetaxel-Loaded MMCNs. The human breast cancer cells (MCF7), cultured in an RPMI-1640 medium supplemented with 10% fetal bovine serum (FBS) and 1% penicillin−streptomycin at 37 °C for 48 h, were used for a cell viability test. The cells were seeded in a 96 well flat-bottom microassay plate at a concentration of 1×10^4 viable cells/well and cultured for 24 h. The MMCNs synthesized using a two liquid phase system by ultrasound irradiation in the absence of isooctane were used for the tests. The MMCNs sterilized with UV irradiation for 12 h were added into wells at a certain concentration and cocultured with the cells for 96 h. The concentrations of the added MMCNs and docetaxel-loaded MMCNs ranged from 0.1 to 500 μg mL^{-1}, while those of free docetaxel ranged from 0.0133 to 66.5 μg mL^{-1} to ensure that the amount of the free drug used was equivalent to that in docetaxel-loaded MMCNs. The drug percentage of docetaxel-loaded MMCNs was 13.3 wt %. The cell viability was quantified by the 3-(4,5-dimethylthiazol-2-yl)-2,5-diphenyltetrazolium bromide (MTT) assay. All reagents used in cell viability experiments were purchased from Sigma Aldrich.

Characterization. The transmission electron microscopy (TEM) micrographs were obtained with a field-emission transmission electron microscope (JEOL, JEM-2100F), equipped with an X-ray energy-dispersive spectrometer (EDS, Oxford instruments, INCA Energy). The X-ray powder diffraction (XRD) patterns were recorded using an X-ray diffractometer (Rigaku, Ultima IV) with a high-intensity Cu Kα radiation (λ = 1.54178 Å) and a graphite monochromator. The magnetic characterization was carried out on a physical property measurement system (PPMS, Quantum Design, USA) at the temperature of 300 K. The nitrogen adsorption−desorption isotherms were performed on a surface area and pore porosimetry analyzer (Gold APP, V-Sorb 2800P, China) at 77 K. Dynamic light scattering (DLS) measurements were measured with a Zeta potential analyzer (ZetaPlus, Brookhaven Instruments Corporation).

RESULTS AND DISCUSSION

TEM micrographs (Figure 1a,b) show that the MMCNs synthesized without isooctane have the core−shell structure. The core consists of the assembly of hydrophobic MIO nanoparticles. The shell is characterized by three-dimensional hierarchical networks of nanosheets, and this structural feature is also confirmed by the SEM micrograph (Figure 1c). The dynamic light scattering (DLS) measurements indicate that the average diameter of MMCNs is 945 ± 96 nm (Figure S1, Supporting Information), which is consistent with the TEM observation. The chemical components of the MMCNs at different sites of a single MMCN were measured by X-ray energy dispersive spectroscopy (EDS) (Figure 1d). In the EDS spectrum, the peaks corresponding to Si and O are clearly observed both at the core (site I) and the shell (site II). However, in contrast with the core site (site I), the peaks corresponding to Fe are absent at the shell site (site II). These results indicate that the chemical components of the core and shell are MIO and CS, respectively.

The proposed formation process of the MMCNs is illustrated in Scheme 2. In the step 1, the hydrophobic phase consisting of tetraethyl orthosilicate (TEOS) and MIO is present on the water phase before the ultrasound irradiation (Scheme 2, Figure S2a in Supporting Information). In the step 2, small hydrophobic drops are formed from the hydrophobic

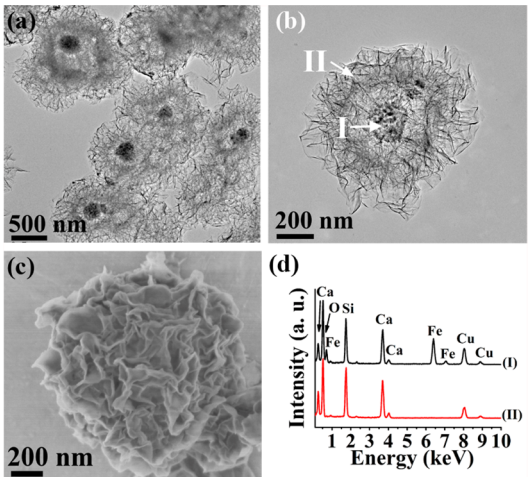

Figure 1. TEM micrographs (a, b) and SEM micrograph (c) of the MMCNs synthesized using a two liquid phase system by ultrasound irradiation in the absence of isooctane. (d) EDS measured at different sites (I and II) of an individual MMCN in (b).

Scheme 2. Formation Process of the MMCNs with the Core/Shell Structure Synthesized Using a Two Liquid Phase System by Ultrasound Irradiation in the Absence of Isooctane

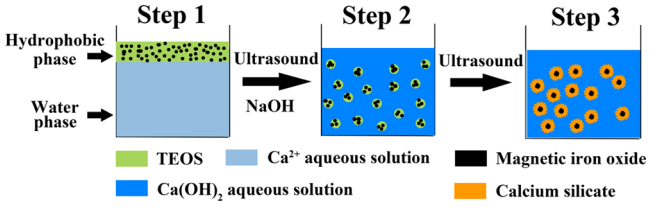

phase under the combined effects of the ultrasound irradiation and the interaction with $Ca(OH)_2$ (formed by the reaction between $Ca(NO_3)_2$ and NaOH). As shown in Figure S2b (Supporting Information), a turbid liquid is formed after ultrasound irradiation for 30 s in contrast to the transparent water phase before irradiation (Figure S2a, Supporting Information). This phenomenon indicates that the small hydrophobic drops are formed and dispersed in water. The hydrophobic phase is gradually divided into smaller drops until the sizes decrease to the smallest under both effects of ultrasound and surface tension. Since the average diameter of MMCNs is ~945 nm, the smallest drops are supposed to be in the range of micrometer to submicrometer. In step 3, $Ca(OH)_2$ in the water phase surrounding the hydrophobic drops reacts with TEOS to produce calcium silicate (CS). It is noteworthy that the heterogeneous nucleation occurs at the phase interface where the chemical reaction occurs. Therefore, the CS shell can initially grow from the outside of small hydrophobic drops and extend into the inside. During the formation of the CS shell, the MIO nanoparticles in the small hydrophobic drops gradually aggregate in the center and self-assemble into the core. Finally, the core−shell structured MMCNs can be obtained after the above three steps.

According to the formation mechanism of MMCNs illustrated above, if the hydrophobic phase is mixed with a certain amount of inert hydrophobic solvent (e.g., isooctane), it will be distributed in the hydrophobic drops under the ultrasound irradiation. Since the shells are formed from the outside to inside of the drops, the hydrophobic solvent will be

encapsulated within the CS shells and take up some space in MMCNs (Figure 2a). Thereafter, due to the solubility of the

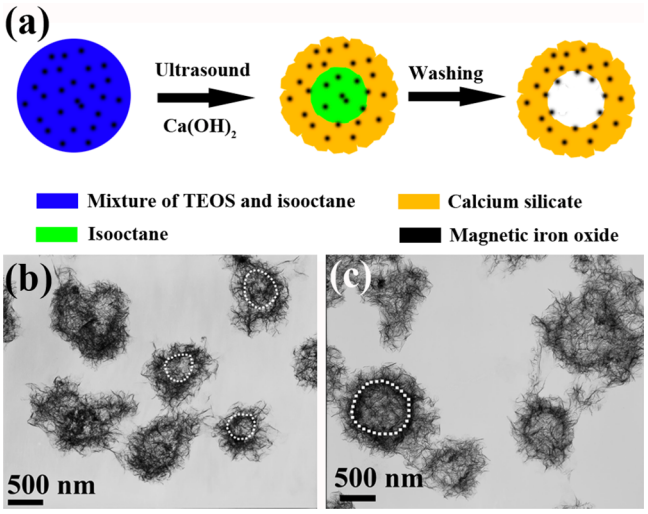

Figure 2. (a) Formation process of the MMCNs with the hollow structure synthesized using a two liquid phase system by ultrasound irradiation in the presence of isooctane. (b, c) TEM micrographs of the MMCNs synthesized using a two liquid phase system by ultrasound irradiation in the presence of isooctane with different volumes: (b) 0.3 mL; (c) 0.6 mL.

hydrophobic solvent in ethanol, the cavity structure will form in MMCNs after the removal of the solvent by washing the product with ethanol (Figure 2a). The results of TEM micrographs confirm this synthetic design (Figure 2). It can be seen that the MMCNs synthesized in the presence of 0.3 mL of isooctane in the hydrophobic phase have the obvious hollow structure (Figure 2b). When 0.6 mL of isooctane is added, the cavities in some MMCNs are so large that part of the MMCN collapses (Figure 2c), and only a small number of MMCNs with a closed hollow structure and thin CS shell are observed. It is found that the MIO cores are rarely clearly observed in MMCNs synthesized in the presence of isooctane. This should be a result of the increased dispersibility of MIO nanoparticles in mixed solvents of TEOS and isooctane, which is confirmed by the fact that the MIO nanoparticles dispersed in the mixture of TEOS and isooctane are much more stable than those in pure TEOS during our experiments. Because of this, the MIO nanoparticles cannot form the self-assembled core but adhere to CS shell and disperse in the added hydrophobic solvent during the formation of MMCNs.

Figure 3a shows the XRD patterns of MMCNs obtained using a two liquid phase system by ultrasound irradiation. It has been found that the MMCNs synthesized without isooctane or with isooctane have the mixed phases of MIO (Fe_3O_4, JCPDS 19-0629) and CS ($Ca_5Si_6O_{16}(OH)_2{\cdot}8H_2O$, JCPDS 29-0331). The XRD results further confirm the chemical components of the MMCNs. The crystal phase of the MIO originates from the addition of preformed MIO nanoparticles (Figure S3, Supporting Information), and the CS phase is formed by the reaction between TEOS and $Ca(OH)_2$. It is noteworthy that the MMCNs synthesized using isooctane have a higher CS crystallinity than that of the sample obtained without isooctane. This may be attributed to the dilution of TEOS by isooctane and the prolonged ultrasound irradiation time. The dilution of TEOS slows down the chemical reaction, and the prolonged

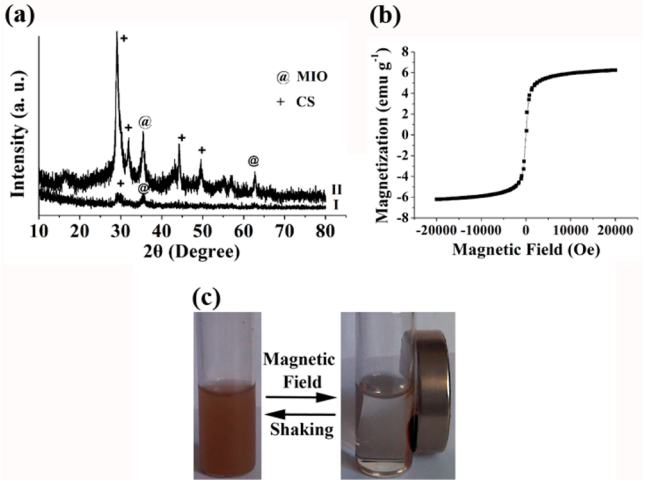

Figure 3. (a) XRD patterns of the MMCNs synthesized using a two liquid phase system by ultrasound irradiation without isooctane (I) and with 0.6 mL isooctane (II); (b) magnetic hysteresis loop of the MMCNs synthesized using a two liquid phase system by ultrasound irradiation without isooctane; (c) magnetic separation–redispersion process of MMCNs in aqueous solution.

irradiation time provides more time for the crystallization of CS.

Figure 3b displays the magnetic hysteresis loop of the MMCNs synthesized using a two liquid phase system by ultrasound irradiation without addition of isooctane. Because of the MIO nanoparticle component, the MMCNs have the superparamagnetic behavior with the saturation magnetization of 6.2 emu g^{-1}. By comparison of the hysteresis loops, we have found that the magnetic property of the MMCNs obtained without using isooctane is similar to that prepared using 0.6 mL of isooctane (Figure S4a,b, Supporting Information). This result indicates that the MMCNs prepared without and with isooctane have similar CS/MIO weight ratios, because the magnetic behavior of the MMCNs is contributed by MIO nanoparticles (Figure S4c, Supporting Information). The MMCNs in aqueous dispersion can be easily separated using a magnet within 1 min and dispersed again by slight shaking, showing good dispersibility and magnetic response in water (Figure 3c).

The nitrogen adsorption–desorption isotherms of the MMCNs were measured to investigate the specific surface area and pore size distribution (Figure 4a,b). All the isotherms can be classified as the type IV (Figure 4a), which is the characteristic of materials with mesopores. The Brunauer–Emmett–Teller (BET) specific surface areas are 164, 474, and 427 m^2 g^{-1} for the MMCNs synthesized without isooctane, with 0.3 mL of isooctane, and with 0.6 mL of isooctane, respectively. As far as we know, few reports on BET specific surface areas of pure CS and its composites were higher than 474 m^2 g^{-1}.[16−18] The structure of the CS shell of the MMCNs, which is formed by the self-assembly of thin nanosheets, should mainly contribute to the high specific surface area. The residual isooctane molecules in the MMCNs prevent the close packing of nanosheets during the CS formation process and further yield more mesopores in the MMCNs. Using the Barrett–Joyner–Halenda (BJH) method, the pore size distributions were investigated with the desorption branch of the isotherms (Figure 4b). For the MMCNs synthesized without isooctane, with 0.3 mL of isooctane, and with 0.6 mL of isooctane, the

dx.doi.org/10.1021/am3021284 | ACS Appl. Mater. Interfaces 2012, 4, 6969−6974

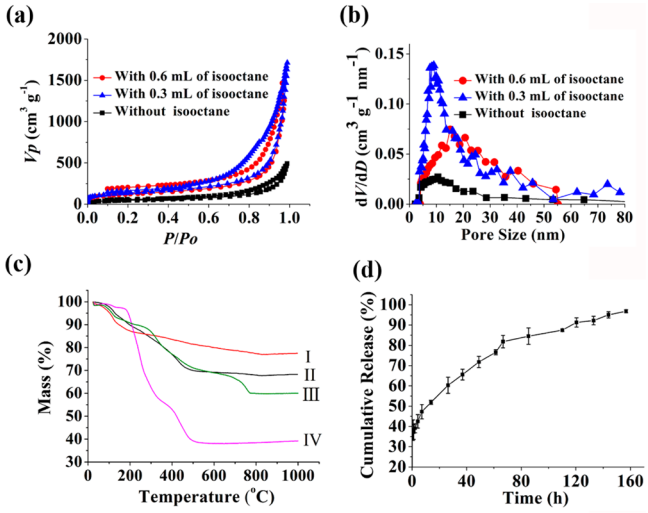

Figure 4. (a) N_2 adsorption−desorption isotherms and (b) BJH desorption pore size distribution curves of the MMCNs obtained using a two liquid phase system by ultrasound irradiation; (c) TG curves of MMCNs without drug (I) and the drug-loaded MMCNs (II: docetaxel; III: bovine hemoglobin; IV: ibuprofen). (d) Docetaxel release profile of the drug-loaded MMCNs in phosphate buffer saline (PBS).

peaks in the pore size distribution curves are shown at 9.5, 9.0, and 15.1 nm, respectively, and the BJH desorption cumulative pore volumes are 0.77, 2.75, 2.18 $cm^3\ g^{-1}$, respectively. According the previous reports, the BJH pore volumes of most calcium silicate materials and their composites were lower than 1.0 $cm^3\ g^{-1}$, and none was higher than 2.0 $cm^3\ g^{-1}$.[16,19,20] Considering ultrahigh specific surface area, pore size distribution, and ultrahigh pore volume, the MMCNs are the ideal candidates for loading drugs with both high and low molecular masses. We also notice that the presence of isooctane has significantly increased the pore volume, although the pore diameter of the MMCNs synthesized using 0.3 mL of isooctane is similar to that obtained without isooctane. This further supports our discussion about the effect of isooctane on the formation of the mesoporous structures.

Ultrahigh specific surface area and pore volume and good magnetic performance enable the MMCNs to have promising potential in magnetically targeted drug delivery. Therefore, the drug loading and release behavior of the MMCNs were studied. Both model drugs with low (docetaxel and ibuprofen) and high (bovine hemoglobin) molecular masses were used to study the drug loading ability. The drug loading capacity for docetaxel, bovine hemoglobin, and ibuprofen, calculated from the thermogravimetric (TG) curves of the pure MMCNs and drug-loaded MMCNs, are 0.153, 0.28, and 1.03 g/g (drug/carrier), respectively (Figure 4c), and these results are consistent with those obtained from the UV−vis analysis (0.12, 0.33, and 0.96 g/g, respectively). These results show that the MMCNs have very high loading capacities for the drugs with both high (hemoglobin) and low (docetaxel and ibuprofen) molecular masses. Furthermore, bovine hemoglobin is soluble in water, while docetaxel and ibuprofen are insoluble in water. In this respect, the above results also confirm that the MMCNs are excellent carriers for loading both hydrophilic and hydrophobic drugs. The ultrahigh drug loading capacity for ibuprofen (1.03 g/g) can be attributed to high specific surface area and chemical interaction between the CS nanocarrier and ibuprofen molecules.[14] In vitro drug release behavior of the docetaxel-loaded MMCNs was investigated in the phosphate buffer saline (PBS, pH = 7.4) at 37 °C (Figure 4d). The docetaxel release from the MMCNs is rapid in the first 6 h, then gradually slows down, and is almost complete at a release time of 160 h.

The cytotoxicity was measured to investigate the biocompatibility and anticancer ability of the MMCNs and docetaxel-loaded MMCNs using human breast cancer (MCF 7) cells. When the cells are cocultured with the MMCNs without loading docetaxel in the concentration range from 0.1 to 500 $\mu g\ mL^{-1}$, no appreciable toxicity is observed. The results indicate that the MMCNs have a high biocompatibility (Figure 5a). In

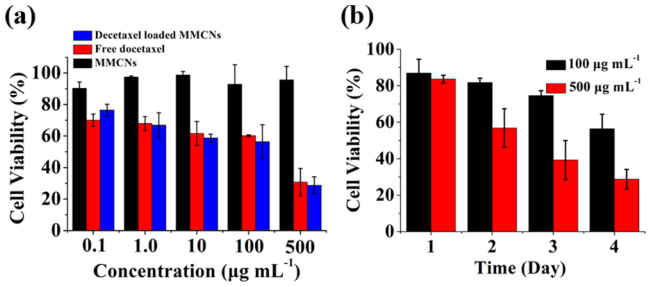

Figure 5. (a) Cytotoxicity tests of the docetaxel-loaded MMCNs with different concentrations for 96 h. The values (0.1, 1.0, 10, 100, 500 $\mu g\ mL^{-1}$) correspond to the concentrations of pure MMCNs and docetaxel-loaded MMCNs. The corresponding concentrations of the free docetaxel are 0.0133, 0.133, 1.33, 13.3, and 66.5 $\mu g\ mL^{-1}$ (to ensure that the amount of the free drug used is equivalent to that in docetaxel-loaded MMCNs). The drug percentage of docetaxel-loaded MMCNs is 13.3 wt %. (b) Cytotoxicity tests of the docetaxel-loaded MMCNs for different times.

the morphological study of the cells treated with MMCNs, nearly all the cells can maintain the spindle shape even at high MMCNs concentration, which stands for active physiological state (Figure 6). However, when the docetaxel-loaded MMCNs is present, the cell viability sharply reduces with increasing concentration (Figure 5a) and the time (Figure 5b). The shapes of the cells also clearly transform from spindle to spherical morphology which is an indication of the inactive state, even at low concentration of the docetaxel-loaded MMCNs (Figure 6). The damage and death of the cells can be attributed to the anticancer drug docetaxel released from the docetaxel-loaded MMCNs. The cell viability of the docetaxel-loaded MMCNs is similar to that of free docetaxel, indicating that the docetaxel-loaded MMCNs have a similar anticancer ability to that of free docetaxel.

The internalization of the MMCNs into the human breast cancer (MCF 7) cells was investigated. Figure S5 in the Supporting Information shows the fluorescence microscopy images of the MCF7 cells cocultured with the fluorescein−MMCNs for 4 h, indicating that the MCF7 cells can internalize the fluorescein−MMCNs. The inset micrographs show the distribution of the fluorescein−MMCNs in an individual cell. The fluorescein−MMCNs can be found on the cell membrane and in cytoplasm. Considering their relatively large sizes, we propose that the active transport process is responsible for the internalization of the fluorescein−MMCNs in the cells. According to the previous reports, the particles with large sizes can be internalized by the cells through the active transport, such as the endocytosis and pinocytosis processes, by

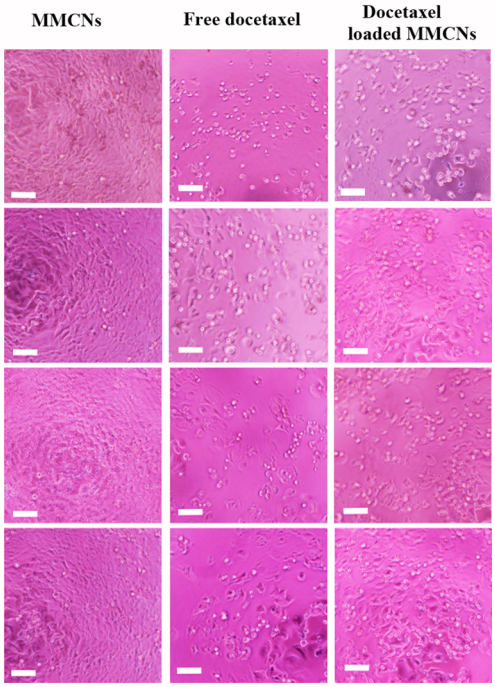

Figure 6. The morphologies of human breast cancer (MCF 7) cells after being cocultured with pure MMCNs, free docetaxel, and decetaxel-loaded MMCNs at different concentrations. From bottom to top, the concentrations of the MMCNs and decetaxel-loaded MMCNs used in the tests are 0.1, 1.0, 10, and 100 μg mL^{-1}; the concentrations of free docetaxel used in the tests are 0.0133, 0.133, 1.33, and 13.3 μg mL^{-1} (to ensure that the amount of the free drug used is equivalent to that in docetaxel-loaded MMCNs). The drug percentage of docetaxel-loaded MMCNs is 13.3%. Scale bar = 100 μm.

which microparticles even with sizes of 1−3 μm can be internalized.[21−23]

CONCLUSIONS

In summary, the core−shell structured mesoporous nanocomposites (MMCNs) consisting of magnetic iron oxide nanoparticles as the core and calcium silicate as the shell have been successfully synthesized using a two liquid phase system by ultrasound irradiation, in which the hydrophobic phase is composed of hydrophobic Fe_3O_4 nanoparticles and tetraethyl orthosilicate (TEOS), and the water phase consists of $Ca(NO_3)_2$, NaOH, and water. When adding a certain amount of a hydrophobic solvent isooctane to the hydrophobic phase, the MMCNs with a hollow structure are obtained. The MMCNs have a good biocompatibility, superparamagnetic behavior, high BET specific surface area (474 m^2 g^{-1}), and ultrahigh BJH pore volume (2.75 cm^3 g^{-1}). The MMCNs have high drug loading capacities for bovine hemoglobin, docetaxel, and ibuprofen. The drug loading capacities for docetaxel, bovine hemoglobin, and ibuprofen are 0.153, 0.28, and 1.03 g/g, respectively. The docetaxel-loaded MMCNs exhibit anticancer ability; thus, they are promising for applications in biomedical fields.

ASSOCIATED CONTENT

Supporting Information

Size distribution of the MMCNs in aqueous solution measured by dynamic light scattering (DLS); the photographs of the two liquid phase systems before and after ultrasound irradiation; XRD pattern of magnetic iron oxide nanoparticles; magnetic hysteresis loops of magnetic iron oxide nanoparticles, the MMCNs synthesized without isooactane, and with 0.6 mL of isooctane; fluorescence microscopy images of the internalization of the fluorescein-MMCNs into human breast cancer (MCF7) cells. This material is available free of charge via the Internet at http://pubs.acs.org.

AUTHOR INFORMATION

Corresponding Author

*Fax: +86-21-52413122. E-mail: y.j.zhu@mail.sic.ac.cn.

Notes

The authors declare no competing financial interest.

ACKNOWLEDGMENTS

This work is supported by the National Basic Research Program of China (973 Program, No. 2012CB933600), the National Natural Science Foundation of China (51172260, 51121064, 51102258), the Science and Technology Commission of Shanghai (11nm0506600), and CAS/SAFEA International Partnership Program for Creative Research Teams.

REFERENCES

(1) Shinkai, M.; Ito, A. *Adv. Biochem. Eng. Biotechnol.* **2004**, *91*, 191.
(2) Laurent, S.; Forge, D.; Port, M.; Roch, A.; Robic, C.; Elst, L. V.; Muller, R. N. *Chem. Rev.* **2008**, *108*, 2064.
(3) Luo, B.; Xu, S. A.; Luo, A.; Wang, W. R.; Wang, S. L.; Guo, J.; Lin, Y.; Zhao, D. Y.; Wang, C. C. *ACS Nano* **2011**, *5*, 1428.
(4) Liu, J.; Qiao, S. Z.; Hu, Q. H.; Lu, G. Q. *Small* **2011**, *7*, 425.
(5) Huang, C.; Zhou, Y. B.; Tang, Z. M.; Guo, X.; Qian, Z. Y.; Zhou, S. B. *Dalton Trans.* **2011**, *40*, 5026.
(6) Wu, H. C.; Wang, T. W.; Bohn, M. C.; Lin, F. H.; Spector, M. *Adv. Funct. Mater.* **2010**, *20*, 67.
(7) Nhiem, T.; Webster, T. J. *Acta Biomater.* **2011**, *7*, 1298.
(8) Jerome, C.; Aqil, A.; Vasseur, S.; Duguet, E.; Passirani, C.; Benoit, J. P.; Roch, A.; Muller, R.; Jerome, R. *Eur. Polym. J.* **2008**, *44*, 3191.
(9) Juríková, A.; Csach, K.; Koneracká, M.; Závišová, V.; Múčková, M.; Tomašovičová, N.; Lancz, G.; Kopčanský, P.; Timko, M.; Miškuf, J. *J. Phys.: Conf. Ser.* **2010**, *200*, 122004.
(10) Ma, W. F.; Wu, K. Y.; Tang, J.; Li, D.; Wei, C.; Guo, J.; Wang, S. L.; Wang, C. C. *J. Mater. Chem.* **2012**, *22*, 15206.
(11) Na, H. K.; Kim, M. H.; Park, K.; Ryoo, S. R.; Lee, K. E.; Jeon, H.; Ryoo, R.; Hyeon, C.; Min, D. H. *Small* **2012**, *8*, 1752.
(12) Jaina, S. K.; Awasthib, A. M.; Jaina, N. K.; Agrawala, G. P. *J. Controlled Release* **2005**, *107*, 300.
(13) Li, H.; Chang, J. *J. Controlled Release* **2005**, *107*, 463.
(14) Wu, J.; Zhu, Y. J.; Cao, S. W.; Chen, F. *Adv. Mater.* **2010**, *22*, 749.
(15) Zhang, M. L.; Chang, J. *Ultrason. Sonochem.* **2010**, *17*, 789.
(16) Su, J.; Wang, Z.; Yan, Y.; Wu, Y.; Cao, L.; Ma, Y.; Yu, B.; Li, M. *J. Nanomater.* **2010**, Art. No. 181429.
(17) Johnston, J. H.; Borrmann, T.; Rankin, D.; Cairns, M.; Grindrod, J. E.; McFarlane, A. *Curr. Appl. Phys.* **2008**, *8*, 504.
(18) Johnston, J. H.; Grindrod, J. E.; Dodds, M.; Schimitschek, K. *Appita J.* **2008**, *61*, 359.
(19) Xue, W. C.; Bandyopadhyay, A.; Bose, S. *Acta Biomater.* **2009**, *5*, 1686.
(20) Zhu, H.; Wu, B.; Feng, X.; Chen, J. *J. Biomed. Mater. Res. B* **2011**, *98B*, 330.
(21) Rejman, J.; Oberle, V.; Zuhorn, I. S.; Hoekstra, D. *Biochem. J.* **2004**, *377*, 159.
(22) Ke, C. J.; Su, T. Y.; Chen, H. L.; Liu, H. L.; Chiang, W. L.; Chu, P. C.; Xia, Y. N.; Sung, H. W. *Angew. Chem., Int. Ed.* **2011**, *50*, 8086.
(23) Foged, C.; Brodin, B.; Frokjaer, S.; Sundblad, A. *Int. J. Pharm.* **2005**, *298*, 315.